Journal of Geotechnical and Transportation Engineering
Volume 4 | Issue 2
The Effect of Tunnel Lining Contact Surface with Medium on Earthquake Dynamic Load Transmission
Basirat et al.
Received 10/12/2018
Published 12/31/2018
Corresponding Author:
Hossein Salari-rad;
salarih@aut.ac.ir
Accepted 11/21/2018
www.jgtte.com

The Effect of Tunnel Lining Contact Surface with Medium on Earthquake Dynamic Load Transmission

Rouhollah Basirat
Faculty of Engineering, Tarbiat Modares University, Tehran, Iran
Email: R.Basirat@modares.ac.ir

Hossein Salari-rad
Mining and Metallurgical Engineering Department, Amirkabir University of Technology, Tehran, Iran
Email: salarih@aut.ac.ir

Hamed Molladavoodi
Mining and Metallurgical Engineering Department, Amirkabir University of Technology, Tehran, Iran
Email: hamedavodi@aut.ac.ir

Seyed Mehdi Hosseini
Civil Engineering Department, Shahrood University of Technology, Shahrood, Iran
Email: S.M.Hosseini@shahroodut.ac.ir

Abstract

For most of the tunnels, the rock-support interface can vary between some full-slip to a non-slip condition, so both types should be investigated for static lining forces and deformations. In dynamic analysis, these conditions have a deterministic role on the interaction between the tunnel periphery rock mass and tunnel lining and evidently, on the load transfer intensity between them.
In this paper, a dynamic analysis of tunnels under different conditions of the rock mass and lining interface has been carried out by analytical and FEM numerical methods. Also, the effect of the interface between tunnel lining and surrounding medium on earthquake intensity studied. In the following, the numerical results are verified based on an analytical method. The numerical and analytical results have a meaningful agreement with themselves. Results also showed that tunnel lining is more confronted with the induced stress due to the earthquake shake forces in non-slip condition, while in medium it is the other way around.

Keywords: Interface, Full-Slip, Non-Slip, Earthquake Loading, Tunnel Lining

1. Introduction

The safety of the underground structures in seismic areas is an important part of the civil engineering projects. The available knowledge about the behavior of tunnels in soft ground during an earthquake loading is limited. By reviewing different case histories can be understand that to increase the reliability of the tunnel structure and to accommodate larger events at closer distances, it is necessary to consider the effect of the dynamic loads generated by earthquakes [1]. Also, there is not adequate certainty in the soil or rock-structure interaction of tunnel and medium.

There are several factors which affect the behavior of tunnels under earthquake loading such as depth of the tunnel below the ground surface, the type of soil or rock surrounding the tunnel, maximum ground acceleration, the intensity of the earthquake, the distance to the earthquake epicenter, and the type of tunnel lining. The relative effects of these factors are unknown but reported cases state that deep underground structures suffer less damage than surface structures [2,3].
So far, several methods have been presented for dynamic analysis of systems maintenance tunnels under dynamic load. These methods are classified into four categories: experimental, quasi-static, analytic, and numerical.
Sun et al. (2011) carried out a model test of the portals of two parallel tunnels to learn about the dynamic response of tunnel liner and the interaction between surrounding rock and liner in earthquakes. Their experiment results showed that when the seismic acceleration traverses the model material, the low-frequency segment of seismic acceleration is magnified, and the high-frequency segment of seismic acceleration is attenuated [4]. Xu et al. (2016) performed a series of three-dimensional shaking table tests to investigate the mechanism and effect of seismic measures of mountain tunnel using a scaled model based on a real tunnel. Their experimental results indicated that installing a geofoam isolation layer between the reinforced surrounding rock and the tunnel lining reduces dynamic earth pressure by 70–90% for the lining without a seismic isolation layer [5]. Hassanzadeh et al. (2018) also investigated the effects of input motion along with structural stiffness properties on seismic behavior of rectangular tunnels [6].
Quasi-static and analytic methods are provided by considering the simplified assumptions including homogeneous and elastic medium and monolithic lining. Some of these methods are Wang [7], Corigliano [8], Park [9], Yi et al. [10], etc. Cao and Yan studied the dynamic response of tunnel with different lining rigidity based

on FEM [11]. Hassani and Basirat presented a new simplified method for dynamic analysis of tunnel lining by combining hyper-static reaction method and analytical methods [12, 13]. Zlatanović et al. investigated the interaction between tunnel lining and soil by using ANSIS software [14]. They compared the results for the cases of dense and loose soil conditions, and their reliability evaluated considerable mutual differences, as well as significant factors influencing tunnel–ground interaction for both cases.

Since the real boundary conditions at the soil-structure interface are unknown, simplified solutions available in the literature for the evaluation of seismic actions generally consider two extreme cases which bound the real situation: the *full-slip* and the *non-slip* conditions [2, 7-9]. It seems that the impact of the interface between tunnel lining and medium on earthquake intensity has not been evaluated sufficiently so far. In this paper, the influence of the interface mechanical behavior between tunnel lining and rock or soil periphery is analyzed based on the FEM.

2. Earthquake Parameters

A wide variety of strong motion parameters are used for earthquake engineering purposes. Some of them describe the amplitude of the motion, the others describe the frequency content or duration. Some of these parameters are influenced by two or three of these important ground motion characteristics. Table 1 indicates which ground motion characteristics strongly influence the various ground motion parameters.

Table 1: Ground motion characteristics that are strongly reflected in various ground motion parameters [15]

Ground Motion Parameters	Ground Motion Characteristic		
	Amplitude	Frequency Content	Duration
Peak acceleration, PHA & PHV	×		
Peak velocity, PHV	×		
Sustained maximum acceleration, SMA	×		
Effective period, Tp	×		
Bandwidth		×	
Central frequency, Ω		×	
Shape factor, δ		×	
Power spectrum intensity, G0	×	×	×
Ground frequency, ωg		×	
Ground damping, ξg		×	
Vmax/amax		×	
Duration, Td			×
rms acceleration, arms	×	×	
Characteristic intensity, Ic	×	×	×
Arias intensity, Ia	×	×	×
Cumulative absolute velocity, CAV	×	×	×
Response spectrum intensity, SI	×	×	
Velocity spectrum intensity, VSI	×	×	
Acceleration spectrum intensity, ASI	×	×	
Effective peak acceleration, EPA	×	×	
Effective peak velocity, EPV	×	×	

A single parameter that includes the effects of the amplitude and frequency content of a strong motion record is the rms (root mean square) acceleration, defined as [15]:

$$a_{rms} = \sqrt{\frac{1}{T_d}\int_0^{T_d}[a(t)]^2 dt} \qquad (1)$$

Where T_d is the duration of the strong motion and a(t) is acceleration. Because the integral in equation (1) is not strongly influenced by large, high-frequency accelerations (which occur only over a very short period of time) and it is influenced by the duration of the motion, the rms acceleration can be very useful for engineering purposes. Its value, however, can be sensitive to the method used to define strong motion duration.

A parameter closely related to RMS acceleration is the Arias intensity, defined as:

$$I_a = \frac{\pi}{2g}\int_0^{\infty}[a(t)]^2 dt \qquad (2)$$

The Arias intensity has units of velocity and is usually expressed in meters per second. Since it is obtained by integration over the entire duration rather than over the duration of strong motion, its value is not dependent on the method used to define the duration of strong motion.

The characteristic intensity, defined as

$$I_c = a_{rms}^{1.5} T_d^{0.5} \qquad (3)$$

is related linearly to an index of structural damage due to the maximum deformations and absorbed hysteretic energy [15].

The frequency content of ground motion can also be described by a power spectrum or power spectral density function. The power spectral density function can also be used to estimate the statistical properties of ground motion and to compute stochastic response using random vibration techniques [15].

3. Analytical Method

The assumption that the induced internal forces are caused by excavation has been removed and replaced with an imposed, external quasi-static loading distribution to simulate the earthquake loading. The relationships derived for the thrust force (*T)* and bending moment (*M)* per unit length of tunnel lining (see Fig. 1) associated with the no-slip condition are the followings [6]:

$$T = \frac{E_s}{2(1+\upsilon_s)}\gamma_{max} r\left(1-\frac{\delta}{3}\right)\cos\left[2\left(\theta+\frac{\pi}{4}\right)\right] \quad (4)$$

$$M = \frac{E_s}{2(1+\upsilon_s)}\gamma_{max} \frac{r^2}{2}\left(1+\frac{\delta}{3}+\varepsilon\right)\cos\left[2\left(\theta+\frac{\pi}{4}\right)\right] \quad (5)$$

In case of the full slip condition these relations become respectively:

$$T = \frac{E_s}{2(1+\upsilon_s)}\gamma_{max} r(1-2\eta)\cos\left[2\left(\theta+\frac{\pi}{4}\right)\right] \quad (6)$$

$$M = \frac{E_s}{2(1+\upsilon_s)}\gamma_{max} r^2(1-2\eta)\cos\left[2\left(\theta+\frac{\pi}{4}\right)\right] \quad (7)$$

where the parameters ε, δ, η are defined by:

$$\varepsilon = \frac{2a\left[1+C^*(1-\upsilon_s)\right]-6\frac{C^*}{F^*}[a+4]}{a[4\upsilon_s-4-a]+3\frac{C^*}{F^*}\{4\upsilon_s+a-6(1-\upsilon_s)[2+a]\}+(1-2\upsilon_s)} \quad (8)$$

$$a = C^*(1-\upsilon_s) \quad (9)$$

$$\delta = \frac{a-2-(4\upsilon_s+a)\varepsilon}{2+a} \quad (10)$$

$$\eta = \frac{F^*(1-\upsilon_s)+6\left(\frac{1}{2}-\upsilon_s\right)}{2F^*(1-\upsilon_s)+6(5-6\upsilon_s)} \quad (11)$$

where $C*$ and $F*$ are:

$$C^* = \frac{E_s r\left(1-\nu_l^2\right)}{E_l A_l\left(1-\nu_s^2\right)} \quad (12)$$

$$F^* = \frac{E_s r^3\left(1-\nu_l^2\right)}{E_l I_l\left(1-\nu_s^2\right)} \quad (13)$$

where r is the average tunnel radius, A_l and I_l are the area and the moment of inertia per unit length of the lining, respectively, E_s, E_l, ν_s and ν_l are the Young's modulus and Poisson's ratio of ground and lining respectively. The parameters $C*$ and $F*$ are the "compressibility" and "flexibility" ratios. They represent a measure of the relative stiffness of the ground with respect to the supporting system (i.e. the lining) under a symmetric and antisymmetric loading respectively. Finally, γ_{max} is the absolute value of maximum shear strain calculated in free-field conditions.

$$\gamma_{max} = \frac{V_s}{C_s} \quad (14)$$

Where Vs and Cs are particle velocity and shear wave velocity, respectively.

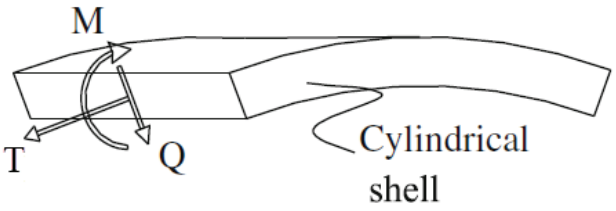

Fig. 1. Internal forces acting on the cylindrical shell in plane strain conditions [8]

4. Numerical Analysis

4.1. Modeling

The numerical analysis has been performed using FEM in PLAXIS Code. The numerical analysis is based on the following assumptions:

a) Plane-strain condition exists.
b) Tunnel lining behave linearly and elastically.
c) Mohr-Coulomb criterion is used for medium behavior.

A 15 node elements and also a fine mesh in geometry of the model were used to obtain higher accuracy. For more accuracy, the meshes around the tunnel are more refined.

Fig. 2 illustrates boundary conditions and seismic loading model. Viscose boundaries are used for dynamic analysis of underground structures and a shear wave that is propagated from the bottom model (Fig. 2).

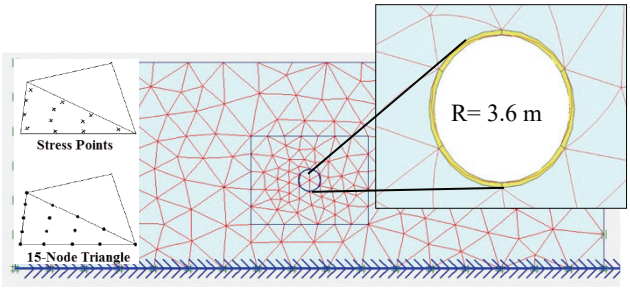

Fig. 2. Numerical model (meshing and boundary conditions)

In this paper, Ab-Golab (water conveyance) tunnel information is selected. The radius of the tunnel is 3.6 m and the thickness of tunnel lining is 25 cm. Overburden in the studied section is 40 meters. Also, the K value (horizontal stress/vertical stress) is considered 0.5 and Mohr-Coulomb criterion is used for medium. Rock mechanics properties of medium at this section are given in Table 2. Lining parameters is also presented in Table 3.

Table 2: Rock mechanics properties of medium [16]

Parameter	Unit	Value
Density	kN/m³	17.5
Elastic Modulus	GPa	1.5
Poisson's Ratio	-	0.26
Cohesion	MPa	0.75
Friction Angle	degree	35

Table 3: Tunnel lining properties

Parameter	Unit	Value
Density	kN/m³	25
Elastic Modulus	GPa	25
Poisson's Ratio	-	0.2
Thickness	cm	25

In this paper, the seismic record which is shown in Fig. 3 are used with a maximum horizontal acceleration of 0.35g. According to Fig. 3, duration of the earthquake is 9 seconds and maximum acceleration occurs between 1.8 and 1.9 (sec).

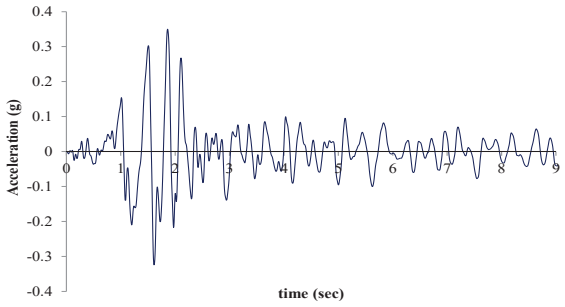

Fig. 3. Earthquake acceleration-time history

4.2. Methodology

In order to investigate the influence of the interface between tunnel lining and surrounding medium, six points are considered in lining and six others in the nearest point on the tunnel lining in medium (Figure 4). After verification of numerical by using analytical method, earthquake intensity calculated in the target points using the provided definitions in section 2 (Figure 5).

According to literatures, interface between the tunnel lining and medium is in fact located in the full-slip (no cohesion) and no-slip (perfect cohesion), so in this paper these conditions are considered [17].

An elastic-plastic model is used to describe the behavior of interfaces for the modelling of soil-structure interaction. The Coulomb criterion is used to distinguish between elastic behavior, where small displacement can occur within the interface, and plastic interface behavior when permanent slip may occur [18].

The stiffness and strength of this interface is determined by the parameter R_{inter}. This parameter relates the stiffness of the interface and the soil through the following relations:

$$C_i = R_{inter} \times C_{soil} \quad (15)$$

$$tan\varphi_i = R_{inter} \times tan\varphi_{soil} \quad (16)$$

Where C_i and ϕ_i are interface cohesion and friction angle, and C_{soil} and ϕ_{soil} are soil cohesion and friction angle respectively [18]. As much as R is closer to 1, the contact between lining and medium is perfected. In this paper R_{inter} is considered 1 and 0.02 for modelling of no-slip and full-slip condition, respectively.

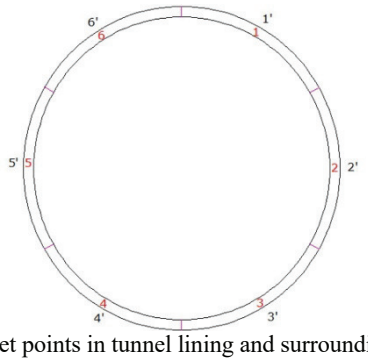

Fig. 4. Target points in tunnel lining and surrounding medium

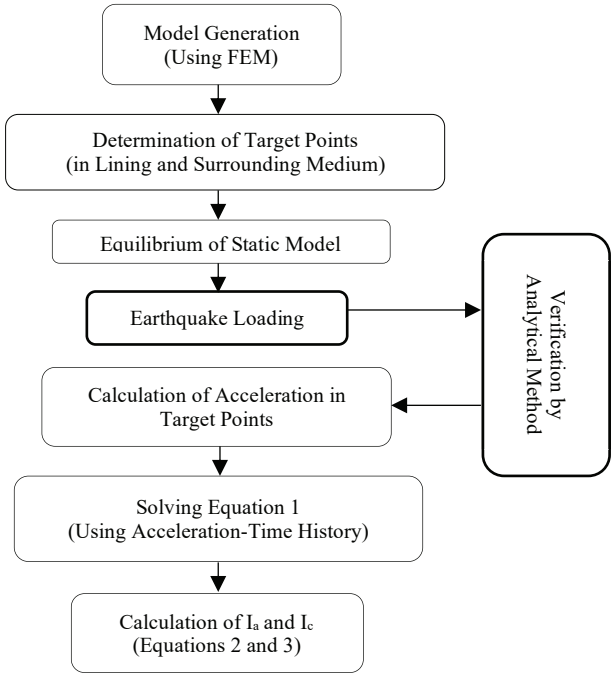

Fig. 5. Methodology of Problem Solution

4.3. Verification

Analytical method was used for verification of numerical method. It should be noted that for verifying the numerical model with analytical method, the medium was considered elastic (Because analytical methods have been developed with the assumption of an elastic medium). After the verification, behavior model changed to the Mohr-Coloumb model. Axial and shear force in lining, due to earthquake load is shown in Figure 6.

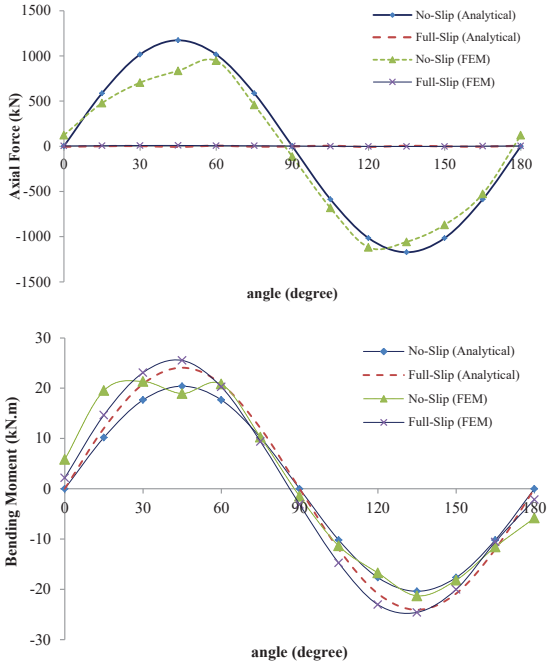

Fig. 6. Axial force and bending moment in lining under earthquake loading

According to this figure, numerical results are in good agreement with analytical method. Based on figure 6 axial force in the no-slip condition is much more than in the full-slip condition, while bending moment in the full-slip condition is a bit more than no-slip condition. This difference is related to stiffness between tunnel lining and medium under two conditions.

5. Study of Numerical Results

Based on acceleration records at the target points, Arias and characteristics intensity parameters in the tunnel lining and surrounding environment are calculated. For example, Arias intensity-time curve is shown for target point 1 in medium in 7. This curve is calculated by acceleration-time history at this point.
Figure 8 indicated the results for the tunnel lining. The average values of the Arias and characteristics intensity in no-slip and full-slip conditions are presented in Table 4.

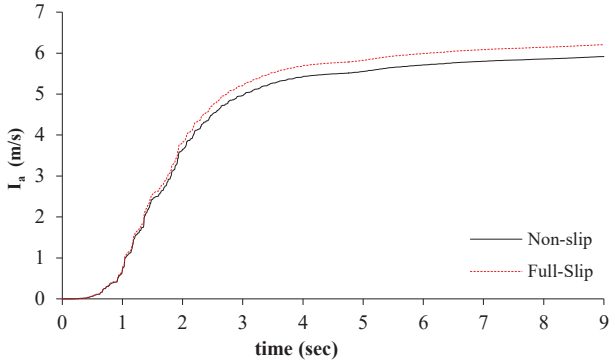

Fig. 7. Arias intensity in medium for target point 1

Table 4: Average values for Arias intensity and characteristic intensity in lining

No-Slip		Full-Slip	
I_a	I_c	I_a	I_c
5.15	6.23	4.95	5.98

Notice: I_a unit is (m/s) and I_c unit is ($\sqrt{[(m/s^2)^3/s]}$)

According to Fig. 8 and Table 4, earthquake intensity in the no-slip condition is more than the full-slip condition. Lack of slip in interface has led to Arias and characteristics intensity in the no-slip is more than the full-slip condition, because lining has full integration with medium and seismic waves have passed through the interface. This makes the stresses in the no-slip condition more than the full-slip condition. The results are in agreement with which some other studies such as references [3, 6, 14].
Fig. 9 demonstrates the results for surrounding medium. The average values of the Arias and characteristics intensity in the no-slip and full-slip conditions are also presented in Table 5.

Table 5: Average values for Arias intensity and characteristic intensity in medium

No-Slip		Full-Slip	
I_a	I_c	I_a	I_c
5.39	6.45	5.66	6.77

Notice: I_a unit is (m/s) and I_c unit is ($\sqrt{[(m/s^2)^3/s]}$)

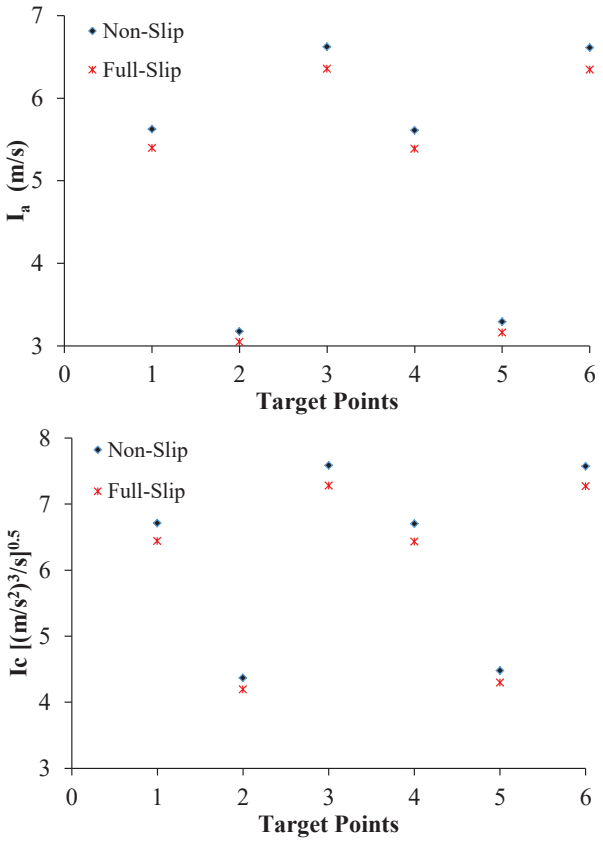

Fig. 8. Arias and characteristic intensity in lining for target points

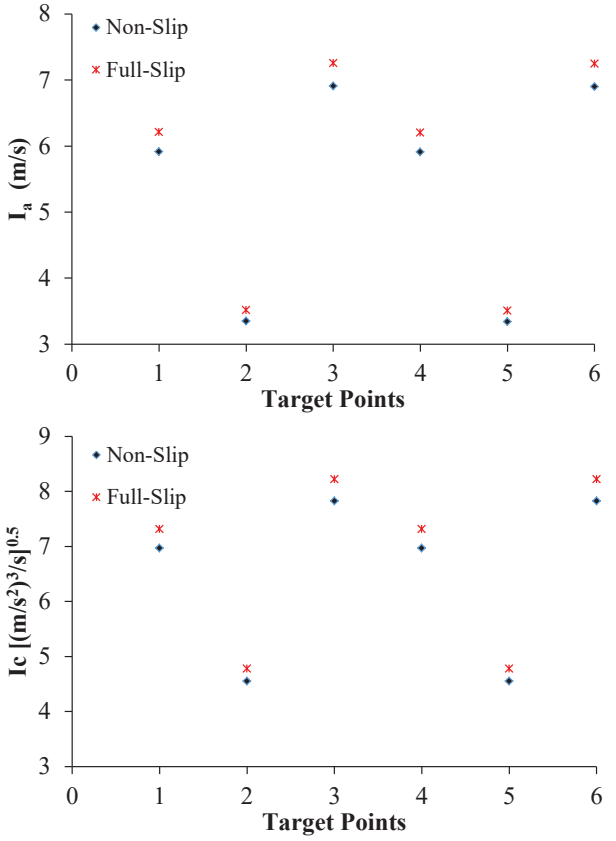

Fig. 9. Arias and characteristic intensity in medium for target points

According to Fig. 9 and Table 5, Arias and characteristics intensity in the full-slip condition is more than the no-slip condition. Therefore, although earthquake intensity in the no-slip condition is more than the full-slip condition in tunnel lining, it is reverse in surrounding medium. Because the lack of cohesion between lining and medium results in incomplete transfer of seismic wave through the interface, and reflection and refraction of the seismic wave in interface increases earthquake intensity in the surrounding medium. As a result, in the full-slip condition, the load of earthquake is mostly imposed on surrounding medium, while in the no-slip condition, this load is divided between tunnel lining and surrounding medium. In other words, in the full-slip condition, more failure happens in the surrounding medium, while in no-slip condition it happens in tunnel lining. However, it is important to note that the lining strength is much higher than the surrounding medium.

6. Conclusion

In this paper, the effect of tunnel lining contact surface with medium on earthquake dynamic load transmission was investigated. Two general conditions for interface, no-slip and full-slip were used. The numerical results were verified by an analytical method. The numerical results were in good agreement with analytical method.

The analysis results showed that axial force in no-slip condition is much more than in the full-slip condition, while bending moment in the full-slip condition is a bit more than the no-slip condition. Results indicated that in tunnel lining the Arias and characteristics intensity in the no-slip condition is more than the full-slip condition, while it is reverse in surrounding medium. Because lack of cohesion between lining and surrounding medium, results in incomplete transfer of seismic wave through the interface, and reflection and refraction of the seismic wave in interface increase earthquake intensity in surrounding medium. Hence, in the full-slip condition more failure happens in surrounding medium, while in the no-slip condition, it happens in tunnel lining.

Therefore, since the surrounding medium's strength is lower than that of the tunnel lining, it is advisable that the contact surface behaves as a no-slip condition with medium. The contact grouting can be used to provide the no-slip condition between permanent tunnel lining and medium. In this situation, the tunnel behaves cohesively with the medium, and finally the more earthquake intensity is occurred in the tunnel lining with the more strength.

References

[1] Jaramillo, C.A., "Impact of seismic design on tunnels in rock – Case histories", Underground Space, 2, 106–114, 2017. DOI: 10.1016/j.undsp.2017.03.004.

[2] Hashash, Y.M.A., Hook, J., Schmidt, B., Yao, J. "Seismic design and analysis of underground structures", Tunnelling and Underground Space Technology Journal, 16(4): 2001, p. 247-293.

[3] Pakbaz, M.C., and Yareevand, A, "2-danalysis of circular tunnel against earthquake loading", J. Tunneling and Underground Space Technology, 20:411–417, 2001.

[4] Sun, T., Yue, Z. Gao, B., Li, Q., Zhang, Y. "Model test study on the dynamic response of the portal section of two parallel tunnels in a seismically active area". Tunnelling and Underground Space Technology, Vol. 26, Issue 2, 2011. DOI: 10.1016/j.tust.2010.11.010

[5] Xu, H., Li, T., Xia, L., Zhao, J.X., Wang, D. "Shaking table tests on seismic measures of a model mountain tunnel". Tunnelling and Underground Space Technology, Vol 60, P 197-209, 2016. DOI: 10.1016/j.tust.2016.09.004.

[6] Hassanzadeh, M., Hajialilue Bonab, M., Javadi, A.A. "Experimental and numerical study of the behavior of shallow rectangular tunnels". Journal of vibroengineering, V. 20, ISSUE 4, 2018. DOI: 10.21595/jve.2018.19308

[7] Wang, J.N., "Seismic Design of Tunnels: A State-of-the-Art Approach", New York, Monograph 7:Parsons Brinckerhoff Quade & Douglas, Inc, 1993.

[8] Corigliano, M. "Seismic Response of Deep Tunnels in Near-Fault Conditions", in Politecnico di Torino,Italy. p. 222, 2007.

[9] Park, K.-H., Tantayopin, K.,Tontavanich, B., Owatsiriwong, A. "Analytical solution for seismic-induced ovaling of circular tunnel lining under no-slip interface conditions: A revisit". J. Tunnelling and Underground Space Technology, 24(2): p. 231-235, 2009.

[10] Yi, C.P., Lu, W.b., Zhang, P., Johansson, D., Nyberg, U. "Effect of imperfect interface on the dynamic response of a circular lined tunnel impacted by plane P-waves", Tunnelling and Underground Space Technology, 51, 68–74, 2016. DOI: 10.1016/j.tust.2015.10.011.

[11] Cao, X and Yan, S. "Numerical analysis for eartquake dynamic response of tunnel with different lining rigidity based on Finite Element Method", Information Technology Journal, Val 12, Pp: 2599-2604, 2013.

[12] Hassani, R. and Basirat, R. "Application of Hyperstatic Reaction Method for Designing of Tunnel Permanent Lining, Part I: 2D Numerical Modelling", Civil Engineering Journal, Vol. 2, No. 6, Pp: 244-253, 2016.

[13] Hassani, R. and Basirat, R. "Application of Hyperstatic Reaction Method for Designing of Tunnel Permanent Lining, Part II: 3D Numerical Modelling", Civil Engineering Journal, Vol. 2, No. 6, Pp: 254-262, 2016.

[14] Zlatanović, E., Lukić, D., Prolović, V., Bonić, Zoran and Davidović, N. "Comparative study on earthquake-induced soil–tunnel structure interaction effects under good and poor soil conditions", European Journal of Environmental and Civil Engineering, 2014. DOI: 10.1080/19648189.2014.992548.

[15] Kramer, S. "Geotechnical Earthquake Engineering", Prentice-Hall, Inc. 653, 1996.

[16] Consultants Rey Water Consulting Engineers (2005) Geology Report of Golab tunnel.

[17] Hashash, Y.M.A., D. Park, and J.I.C. Yao, "Ovaling deformations of circular tunnels under seismic loading, an update on seismic design and analysis of underground structures", J. Tunnelling and Underground Space Technology. 20(5): p. 435-441, 2005.

[18] Brinkgreve R. B. J., and Swolfs W. M. "Plaxis Reference Manual, Version 8" PLAXIS bv, Netherland, 2006.